Numerical Solutions of the Upper Critical Depth Problem

Robert M. Hall* and M. Holt†
University of California, Berkeley, Calif.

The phenomenon of upper critical depth occurs when a spherical charge of explosive is detonated near the surface of the ocean or other large body of water. For different depths of charge center it is found that the maximum surface wave resulting from the explosion corresponds to a position approximately one half charge radius below the surface. The wave amplitude for this position is far larger than for higher or lower positions of the charge. The phenomenon has been explained qualitatively by Sakurai. He considers that the impulse applied to the water is mainly responsible for the effect, since a net downward impulse results only if the charge is partially, rather than totally, submerged. To explore Sakurai's hypothesis in more detail a model of a near ocean surface explosion is proposed in the present paper. The model problem is then solved numerically using a technique due to Godunov for different depths of charge. The impulse applied to the water is calculated as a function of time in each case. The full Godunov scheme uses two half time steps, the first employing a characteristics scheme, and the second a cell type scheme. in the present paper a modified form of the first half of the scheme is used.

Nomenclature

A	= wave speed in model equation
$a_n, b_n, ..$	= coefficients in difference equations
h	= space step
m	= time step index
n	= space step index
p	= pressure
Q	= area factor
t	= time
u	= velocity
v	= network velocity
x	= distance
x', t'	= independent variables in moving system
α	= stabilizing parameter
ρ	= density
τ	= time step

Introduction

WHEN a charge is detonated in water, surface waves may be generated. The shock wave which propagates out from the explosive products will be imparting energy to the water in the form of heat and kinetic energy. Whether or not surface waves are generated by the underwater detonation depends upon the existence of a mechanism to transfer energy of the explosion into energy for surface waves. From the classical solutions to wave propagation problems, the two initial conditions which will produce waves are displacement and velocity. Hence when a charge is detonated in water, surface waves will be created either if the surface is displaced, or if an impulse is applied to the surface. An explosive source of surface wave generation is shown in Fig. 1. Figure 1 shows the variation of wave amplitude with depth of placement for a typical set of detonations using charges of equal size. This amplitude represents the greatest height of a travelling surface wave recorded by an instrument at some distance from the charge center. As seen in Fig. 1, the wave amplitude has two maximum values.

The smaller of these occurs at the lower depth, and results from a displacement effect. After the charge detonates, the explosive products form a very hot, high pressure gas bubble which will push out against the water and expand. As the bubble does work against the water, the inertia of the water will increase, and eventually cause the bubble radius to increase beyond its equilibrium value. If the bubble is far from the surface, and if it does not break down due to instability, it may actually oscillate back and forth many times. However, if the depth of charge placement is such that the bubble has just expanded to its first maximum radius as it strikes the surface, then the largest possible void is formed in the water and this gives rise to the maximum displacement initial condition. The charge position corresponding to this lower wave maximum is called the lower critical depth.

The larger wave maximum occurs within a charge diameter or so from the surface, and the corresponding charge position is called the upper critical depth. The important quantity in this case is the impulse, or velocity, applied to the water rather than the initial displacement.

Sakurai[1] claims that the mechanism for the upper critical depth effect is the impulse imparted to the water. In his paper he makes two important observations. Firstly, since upper critical depth occurs so close to the air-water surface, the explosive products will exert a net impulse on the water body. Secondly, using the technique of Sedov,[2] he carries out a similarity analysis for a strong blast by taking I_0, the impulse, rather than E_0, the energy, as one of the two basic parameters. He finds that the observed expansion of the cavity radius is predicted by the impulse parameter shock

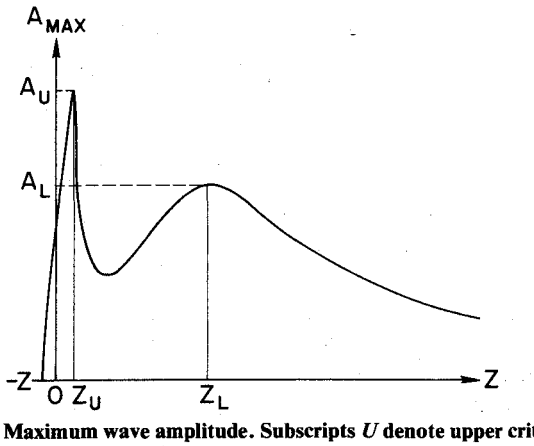

Fig. 1 Maximum wave amplitude. Subscripts U denote upper critical depth while L denotes lower critical depth.

Presented as Paper 75-52 at the AIAA 13th Aerospace Sciences Meeting, Pasadena, Calif., January 20-22, 1975; submitted January 9, 1975.

Index categories: Shock Waves and Detonations; Hydrodynamics; Wave Motion and Sloshing.

*Presently NASA Langley Research Center, Va. Member AIAA.

†Professor, Dept. of Mechanical Engineering. Associate Fellow AIAA.

analysis. Both of these observations by Sakurai make an extremely convincing argument for the importance of impulse in the problem of upper critical depth.

A second paper of importance is that of Bjork and Gittings.[3] Their paper includes a complete numerical solution of the underwater explosion problem for a charge placed at a particular depth. The calculation and plots presented proved to be quite helpful in the formulation of the physical model presented in the present work.

In the present paper a simple model of a near surface explosion is proposed, and a numerical technique is described to calculate the disturbance from the model explosion under various initial conditions. The numerical technique is based on a recent method of Godunov[4] which has been applied to a series of wave propagation problems in Hydraulics, Gas Dynamics, and Plasma Dynamics. Previously this method has only been applied to one-dimensional flow and a prerequisite to using the method for the model explosion problem is to extend it to spherical and three-dimensional geometry. The extension has been completed for the first half of the Godunov scheme, which can be used as it stands provided the total number of time steps is limited. Results of applying the partial scheme to the model problem are presented here, and show the nature of the disturbance, including impulse distribution, at early times. The impulse data can be introduced into a Krantzer-Keller analysis of surface wave motion. This has been reformulated here, with the model problem in mind, by Rosen.[5]

Work is now in progress to add the second half of the Godunov scheme (an explicit corrector step) for general geometry. The full scheme has been used successfully for the plane shock problem in this paper. The full scheme is to be applied to the model problem, to follow the disturbance up to late times for a series of depths of center of charge. The complete scheme will permit a full numerical investigation of the upper critical depth phenomenon. This will also permit a comparison of the present method with the approach of Bjork and Gittings.[3] The latter is an elaborate scheme combining a one-dimensional Lagrangian code with a two-dimensional Eulerian code. It requires a considerable amount of computer time, and its application has been confined to two specific configurations; one for a chemical charge, the other for a nuclear explosion. The Bjork-Gittings calculation provides more information than is needed to verify the upper critical depth phenomenon, and the cost of using it for a series of charge depths and outputs would be prohibitive. With the model problem proposed here this parametric study will be relatively inexpensive. For a general description of explosion generated waves the reader is referred to Whitham[6] and Friedman.[7]

Physical Model

When constructing the model of a physical problem, its degree of complexity will be dictated by certain basic features which have to be taken into account. In the present problem we seek a model which is both simple to construct and economical to apply. The problem has therefore been simplified in such a manner that the true axisymmetric, time dependent problem of an explosion near the surface could be reduced to a pair of time dependent problems in 1 space variable. In addition, it was decided to focus on Sakurai's hypothesis that the impulse imparted to the water is the dominant feature of the upper critical depth problem.

Impulse can either be defined as change of momentum or, equivalently, as force multiplied by time. In fluid mechanics problems the force is usually the result of pressure acting on an area. Since force is a vector and both the pressure and area are scalars, one must associate a direction with the normal to the surface area upon which the force acts. That is,

$$f = p\,A$$

where f is the resultant force, p is the pressure acting on the area, and A is defined as

$$A = A\,n$$

where A is the area of the surface, and n is the unit normal to the surface.

Corresponding to the two equivalent interpretations of impulse, there are two equivalent methods for determining the impulse applied to a fluid region. For example, if we consider a steam driven piston moving into a constant cross-section tube, we may calculate the impulse imparted to the fluid by solving the equations of motion in the entire flow region. While the piston is driven by a constant pressure, the shock is moving ahead at constant velocity. However, as soon as the pressure behind the piston falls, the velocity of the piston begins to decrease. As the resulting rarefaction waves catch up with the shock wave, this too will begin to slow down. At this stage we may use an appropriate characteristics method to determine the fluid behavior in the region between the piston and the shock. By summing the change in the momentum of the fluid region, the impulse imparted to the fluid may be found.

The impulse applied to the fluid in the previous piston problem may also be calculated in another manner. Taking the second definition of impulse, we may direct attention to the pressure exerted by the piston on the fluid. The force is equal to the pressure at the piston multiplied by the tube cross-section. Hence, if the pressure is known at the piston as a function of time, the total impulse imparted to the fluid is the integral of the pressure force over time. Consequently, if we consider a problem in which the pressure over a region is given as a function of time, it is not necessary to solve the equations of motion in that region to determine the impulse applied to it.

In fact, in the upper critical depth problem the impulse imparted to the water results from the pressure exerted by the explosive products. Thus the impulse can be found without solving the equations of motion in the water region if the behavior of the cavity formed by the explosive products (the piston in the upper critical depth problem) can be calculated.

The purpose of the model developed in this paper is to approximate the complicated two-dimensional, unsteady flow of the explosive products in the actual physical problem by a hot gas bubble. This is to grow in time with a shape simulating the observed form of the physical cavity. The cavity refers to the region of the flowfield formed by the hot gas products. Inside the axisymmetric model cavity a one-dimensional unsteady grid is introduced, oriented so that the fluid velocity is restricted to move only in the vertical z direction. As the shape of the cavity changes in time, the one-dimensional unsteady equations of motion will be used to estimate the pressure distribution inside the cavity, and its shape, the net force applied to the water, can be calculated.

Modelling the Detonation

The first simplification introduced in the model is to substitute a sphere of high pressure, high temperature gas for the physical explosive charge. Hence the chemical energy liberated in the explosion process is replaced by high internal energy of the hot gas sphere. This substitution has been made in previous papers by Ballhaus, and Holt[8] and by Chan, Holt, and Welsh.[9]

Modelling the Geometry of the Cavity

The procedure for specifying the behavior of the cavity boundaries depends upon the assumptions made about its shape. It also depends on the rate at which the shape is growing. A typical cavity shape as found from the procedure to be described below is shown in Fig. 2. For ease of description the cavity is divided into four regions—top of the chimney, the chimney, the intermediate region, and the

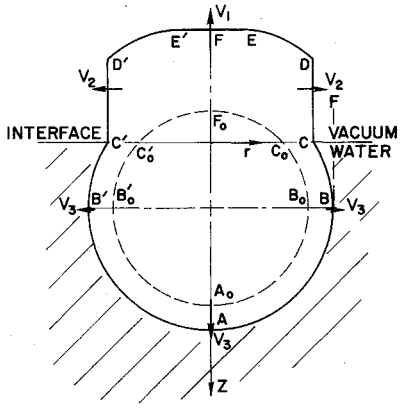

Fig. 2 Cavity shape. Top of chimney—DEFE'D', Chimney—CDD'C', Intermediate region—CBB'C', Hemispherical region—BAB'.

hemispherical region. The determination of the motion of the boundaries of these regions will be described presently.

The top of the chimney follows the hot gas venting into the atmosphere. In this paper the atmosphere has been replaced by a vacuum. Consequently, the fluid in the top of the chimney is travelling vertically upward at the head of the rarefaction wave. The rarefaction wave is the mechanism for release of the pressure inside the cavity. The shape of the top of the chimney is calculated from the initial above-water section of the hot gas bubble, $C_0'F_0C_0$ in Fig. 2. This initial dome is allowed to split apart in the middle and expand in the r direction at the velocity of the expanding chimney.

The results of Bjork and Gittings[3] can be used to help define the behavior of the chimney region. They show that the explosive products which are venting into the atmosphere are travelling into a chimney formed by a water lip. At early times this chimney has nearly constant cross-sectional radius along the z-axis as it expands in time. This assumption of constant cross-section along the z-axis has certain limitations. Certainly, as the charge depth of placement is decreased to zero, we would expect a spherical expansion of the explosion products into the atmosphere. Nevertheless, for a depth of placement of one-half the initial bubble radius or greater, the constant cross-section chimney assumption is reasonable. To deal with very small depths of placement, we could add an appropriate increase in chimney cross-section in the vertical upward region (negative z-direction) to simulate spherical expansion.

Having defined the shape of the chimney, we next determine how quickly it is expanding in the r direction. In the initial bubble configuration there is a water lip which covers part of the gas bubble. (See Fig. 2). As might be expected, once the bubble is released, this water lip is actually thrown upward and outward by the hot gas products. The movement of this lip is crucial because its radius r_L measured from the centerline of the cavity, determines the width of the throat of the chimney region.

To calculate the speed with which the lip peels back, a control volume of water is established in the lip region. This consists of a ring of water which is initially resting on top of the spherical charge, and is a volume of revolution swept out by the cross-section BCF in Fig. 2. The mass of this control volume is taken to be the product of the density of water and its volume. The forces on the volume of revolution are precisely the pressure forces on the various sides of its three surfaces. The pressure above the triangle is taken to be zero since the model replaces the atmosphere by a vacuum. Only two sides, BF and BC, of the ring experience pressure forces. As a first-order approximation to the pressure distribution along BF, assume that the pressure decreases linearly from B to F. Then the average pressure along this line is half the pressure at B. The lateral acceleration of the ring away from the center axis will become

$$a=(p_{BC}-p_B/2)/m\,A_L$$

where m = mass, p_{BC} = a representative pressure along BC, p_B = pressure at B, and A_L = lateral area.

Initially the lip of water is bounded by the upper part of the submerged charge surface, by the ocean surface, and by a vertical cylinder touching the charge sphere. subsequently it accelerates with horizontal component a, so that the inner radius of the lip (radius of chimney) is given by integrating

$$\frac{dx}{dt}=V_i+\int_0^t a\,dt'$$

where V_i is the mean horizontal component of the initial spherical bubble velocity, equal to the escape velocity. When the ring radius equals that of the spherical bubble, it moves with the sphere, so that the disturbed region is bounded by a hemisphere-cylinder.

The intermediate region is defined as the region between the surface plane, $z=0$, and the center of the hemispherical region, z = depth of placement. The rate of radial expansion of this region as a function of z is taken to be a linear combination of the velocity of expansion v_2 at point C and v_3 at point B in Fig. 2. This intermediate rgion is intended to provide a smooth transition from flow in the hemisphere to flow venting out of the chimney.

The hemispherical region is the lower portion of the cavity. Again referring to Fig. 2, one may see that the lower portion of the cavity retains a hemispherical shape. Consequently, motion of the lower portion of the model cavity is a hemisphere which expands at a rate v_3 determined by an auxiliary computer program. This will be described in the following section.

In developing a procedure to specify the shape of the cavity, two clues were taken from the work of Bjork and Gittings.[3] Firstly, the chimney radius was taken to be independent of z. Secondly, the bottom portion of the cavity remains hemispherical as time progresses. In addition, a control volume of water was used to estimate the rate of expansion of the cavity chimney. Hence the shapes of the surfaces and their rates of expansion are used to predict the evolution of the cavity boundaries in time.

Modelling the Interaction between the Cavity and the Water Body

As already mentioned, the model predicts the velocity, v_3 (Fig. 2), of the boundary between the cavity and the water region. This prediction is based on the observation that the bottom portion of the cavity remains nearly hemispherical as time progresses. Consequently, the water below the cavity is acting as though it were a spherically symmetric water problem.

With the above assumptions the movement of the hemispherical region of the cavity is handled as follows. The pressure at point A in Fig. 2 is calculated by the numerical scheme inside the cavity for a particular time, t_o. This value of the pressure is then passed to an auxiliary spherically symmetric water program. The water program can be described as a spherical piston problem in which the pressure at the piston is specified instead of the velocity. With a given value of pressure at the spherical piston, the water program predicts a new value of velocity for the pressure piston. This value of velocity is then returned to the cavity program as the velocity v_3 of the boundary of the hemispherical region. With v_3 specified the new cavity geometry may be calculated, and the cavity program is run again at time $t_o+\tau$. This then predicts a new value of pressure at point A, which is once more transferred to the auxiliary water program. Figure 3 shows symbolically how the cavity and the water program interact.

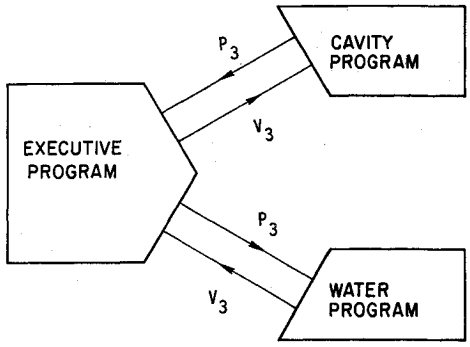

Fig. 3 Program Interaction. P_3 is pressure at bottom of cavity; V_3 is velocity at bottom of cavity.

Numerical Method

The numerical method used for the calculations in the upper critical depth problem is a one step, implicit, finite difference scheme using the characteristic equations in a moving cell network. The basic formulation was taken from a paper by Godunov et al.,[4] in which a new numerical method is presented for solving one-dimensional, inviscid, unsteady flows. This consists of a two step procedure in which the first step is solved by an implicit, characteristic method. The results of this are then smoothed by a parameter, α. The second step uses an explicit finite difference method based on the conservation equations in integral form.

The scheme is unconditionally stable and is of second-order accuracy in both time and position. An important feature of the new Godunov scheme is that of fitting the coordinate system to discontinuities in the flow field. He proposes straining the moving coordinate system in such a manner that external and internal shocks or contact discontinuities are followed by the cell network. The flow is divided into regions between each discontinuity, and each region has its own cell network. The advantage of following a discontinuity such as a shock is that the shock equations themselves may be used to pass across the shock. This preserves the proper jumps in velocity and pressure, and does not smear the change in pressure over many cells.

The Model Equation

Godunov's basic procedure can best be explained and analyzed by examining the model equation

$$\frac{\partial u}{\partial t} + A\frac{\partial u}{\partial x} = 0 \tag{1}$$

where A is a constant, t is the time, and x is the distance along an axis. The model equation grid network is shown in Fig. 4. At grid points $u(x,t)$ is written as

$$u(nh,m\tau) = u_n{}^m$$

where h is Δx, and τ is the time step.

To begin the method all the values of u_n must be specified at a particular time level $t = m_0\tau_0$. One time cycle will be completed when we have calculated the new values of u_n at time $t = (m_0+1)\tau$. Godunov's first step is to calculate values of $u_n^{m+\frac{1}{2}}$—values of u at the integral values, n, of grid position but at a half τ time level. This first step uses the following implicit formula

$$\frac{u_n{}^{m+\frac{1}{2}} - u_n{}^m}{\tau/2} + A\frac{u_{n+1}{}^{m+\frac{1}{2}} - u_{n-1}{}^{m+\frac{1}{2}}}{2h} = 0 \tag{2}$$

Equation (2) has second-order accuracy in the space variable. It is solved by a double sweep between the left boundary $n=1$ and the right boundary $n=N$. The boundary value of $u_1{}^{m+\frac{1}{2}}$ must be specified if A is positive, and for $n=N$ the centered difference is replaced by a simple difference between u_N and u_{N-1}.

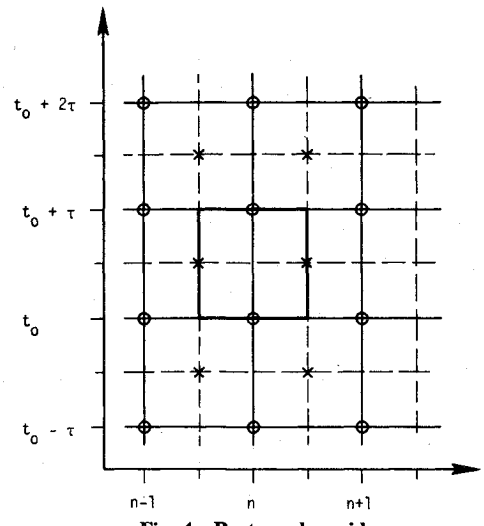

Fig. 4 Rectangular grid.

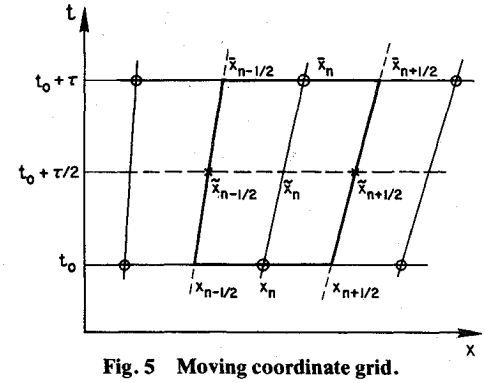

Fig. 5 Moving coordinate grid.

With $u_n{}^{m+1}$ known for all n, values of $u_{n+\frac{1}{2}}{}^{m+\frac{1}{2}}$ are calculated by a smoothing interpolation formula

$$u_{n+\frac{1}{2}}{}^{m+\frac{1}{2}} = (1-\alpha)\frac{u_{n+1}{}^{m+\frac{1}{2}} + u_n{}^{m+\frac{1}{2}}}{2} + \alpha\frac{u_{n+2}{}^{m+\frac{1}{2}} + u_{n-1}{}^{m+\frac{1}{2}}}{2} \tag{3}$$

Godunov proposes the value $\alpha = 0.25$.

With the values of $u_{n+\frac{1}{2}}{}^{m+\frac{1}{2}}$ known the second step in the calculation uses the value of $u_n{}^{m+1}$ from

$$\frac{u_n{}^{m+1} - u_n{}^m}{\tau} + A\frac{u_{n+\frac{1}{2}}{}^{m+\frac{1}{2}} - u_{n-\frac{1}{2}}{}^{m+\frac{1}{2}}}{h} = 0 \tag{4}$$

An analysis of the combined truncation error in the two step procedure shows that the scheme is accurate to order τ^2, h^2. It can also be demonstrated that the scheme is unconditionally stable for any time step, provided $0 < \alpha \leq 0.25$.

Equations of Fluid Mechanics

The scheme for fluids problems and movable networks is described in Godunov.[4] The grid network is allowed to move and deform as shown in Fig. 5. All variables are given for some basic time $t = t_0$. As with the model equations the variables at the new time step $t = t_0 + \tau$ are calculated in two half steps. In the first step the equations of motion are written in characteristic form and differenced in an implicit manner. The results are then smoothly interpolated as before. Finally,

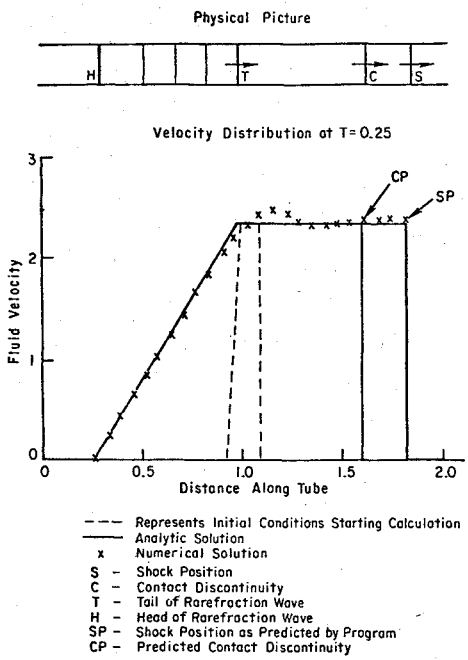

Fig. 6 Air-Air planar shock tube calculation.

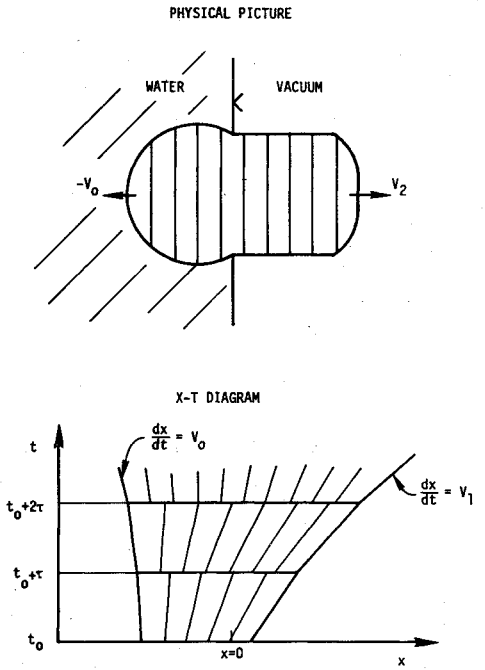

Fig. 7 Moving grid in cavity.

the equations of motion are integrated around a basic cell to give explicit formula for the variables on the new time level $t=t_0+\tau$.

Boundary Conditions

Godunov considers both internal and external types of boundaries. The internal boundary arises in the case where there is a flow discontinuity inside the domain of calculation. For example, there may be an internal shock wave or perhaps a contact discontinuity. In such problems the domain of calculation is broken into continuous regions, each having its own moving grid network. The end of each of these networks is constrained to move with the internal boundary at one end, while it follows the appropriate external, or another internal boundary, at the other end. After isolating the flow discontinuities at the ends of a network region, we may choose the proper physical equations to traverse the discontinuity.

For example, consider the problem of a piston moving into a tube from the left side. Along the piston path the velocity of the piston is specified as a function of time. Entropy at the piston is a constant. Thus there are two boundary conditions for the three unknowns in the first half step. An additional relation is taken from either a $u+c$ or $u-c$ characteristic where u is the velocity, and c is the local speed of sound. The characteristic chosen is that originating inside the grid region and propagating out to the boundary during the half time step. In the present example the $u-c$ characteristic is written with a simple forward difference approximating the x derivatives. There are now three equations for the three unknowns at $n=1$. The right hand side of the grid network in the piston problem follows the resulting shock wave. At the shock wave we have four unknowns—u, p, S, and U_s. U_s is the shock velocity, and is required for proper movement of the grid network. The shock relations yield three equations and the fourth relation is again obtained by choosing a characteristic which originates inside the flow region, and propagates out to the shock. In this case the $u+c$ characteristic relation is chosen.

Simple Applications of the Godunov Scheme

We were able to get satisfactory performance out of Godunov's full, two step procedure for several different problems. However, for particular cases of boundary conditions (the head of a strong, planar rarefaction wave or at the center of a sphere) the numerical scheme presented difficulties.

One problem successfully solved by the two step method is the air-air plane shock tube. High pressure air is separated from ambient air by a diaphragm at position $x=1$. The diaphragm pressure ratio is taken to be 30 and the density of the high pressure air is five times as large as the density of the air to the right. The numerical results are shown in Fig. 6. (The velocity is nondimensionalized such that the sound speed in the ambient air equals 1.183.) The graph shown was made after six time steps.

Moving Cell Network

In many fluid dynamics problems it is desirable to attach the ends of the grid network to the various discontinuities of the flow. For example, in the present model of the underwater explosion cavity, one end of the grid is attached to the contact discontinuity between the cavity and the water. (See Fig. 7.)

One must necessarily incorporate into the difference equations the information that the grid is moving. At the beginning of each time step in the numerical scheme, an equally spaced grid network is placed in each flow region. Applying a new grid at each time step allows more cells to be added if the region of interest is growing. This equally spaced grid at some time, t_0, forms a reference coordinate system. From the previous time step the velocities at the ends of each region are known. In Fig. 7 the right side of the cavity moves at the velocity of the gas escaping into the water at the velocity prescribed by the physical model. Since the ends of the moving grid network are tied to each boundary of the region, the right end of the grid network moves with the same velocity as the gas venting into the atmosphere. The left end of the cavity grid moves with the velocity of the hot gas and water contact discontinuity. The velocities of the internal points of each moving grid network are found by a linear interpolation between the two end velocities of the regions. In Fig. 7 notation this is expressed by

$$v(x)=v_0+(x-x_0)\,(v_1-v_0)/(x_1-x_0) \tag{5}$$

The moving coordinate grid variables, x' and t', may be related to the reference coordinate variables, x and t, by

$$x' = x-v(x)\cdot\delta t \tag{6}$$

$$t' = t \tag{7}$$

$$\delta t = t-t_0$$

where δt is the elapsed time since the beginning of the time step.

In the reference coordinates, the characteristic equations of motion may be written as

$$\left(\frac{\partial u}{\partial t}+\frac{1}{\rho c}\frac{\partial p}{\partial t}\right)+(u+c)\left(\frac{\partial u}{\partial x}+\frac{1}{\rho c}\frac{\partial p}{\partial x}\right)$$

$$=-\frac{uc}{Q}\frac{\partial Q}{\partial x}-\frac{c}{Q}\frac{\partial Q}{\partial t} \tag{8}$$

$$\left(\frac{\partial u}{\partial t}-\frac{1}{\rho c}\frac{\partial p}{\partial t}\right)+(u-c)\left(\frac{\partial u}{\partial x}-\frac{1}{\rho c}\frac{\partial p}{\partial x}\right)$$

$$=\frac{uc}{Q}\frac{\partial Q}{\partial x}+\frac{c}{Q}\frac{\partial Q}{\partial t} \tag{9}$$

$$\frac{\partial S}{\partial t}+u\frac{\partial S}{\partial x}=0 \tag{10}$$

Here Q is an area factor, $Q=r^j$ ($j=0$ for plane symmetry; $j=1$ cylindrical symmetry; and $j=2$ spherical symmetry.) Transforming the left-hand side of Eq. (8) to moving coordinates leads to

$$\left(\frac{\partial u}{\partial t'}+\frac{1}{\rho c}\frac{\partial p}{\partial t'}\right)+\left[(u+c)\left(1-\frac{dv}{dx}\delta t\right)-v\right]\left[\frac{\partial u}{\partial x'}\right.$$

$$\left.+\frac{1}{\rho c}\frac{\partial p}{\partial x'}\right]=-\frac{uc}{Q}\frac{\partial Q}{\partial x}-\frac{c}{Q}\frac{\partial Q}{\partial t} \tag{11}$$

$$\left(\frac{\partial u}{\partial t'}-\frac{1}{\rho c}\frac{\partial p}{\partial t'}\right)+\left[(u-c)\left(1-\frac{dv}{dx}\delta t\right)-v\right]\left[\frac{\partial u}{\partial x'}\right.$$

$$\left.-\frac{1}{\rho c}\frac{\partial p}{\partial x'}\right]=\frac{uc}{Q}\frac{\partial Q}{\partial x}+\frac{c}{Q}\frac{\partial Q}{\partial t} \tag{12}$$

$$\frac{\partial S}{\partial t'}+\left[\left(1-\frac{dv}{dx}\delta t\right)u-v\right]\frac{\partial S}{\partial x'}=0 \tag{13}$$

where Q is still calculated in terms of x, rather than x'.

Numerical Method used in the Present Calculation

Because of the difficulty in formulating proper boundary relations for the full two step Godunov scheme, only the first step was retained. An analysis of the model equation shows that for the implicit step the difference equations are of second-order accuracy in position, and of first-order accuracy in time. The stability analysis of the model system shows that the implicit step is unconditionally stable for any time step.

The differencing is handled in the same manner as for Godunov's first step. The difference equations are

$$a_n\bar{u}_{n+1}+\lambda_n a_n\bar{p}_{n+1}+\bar{u}_n+\lambda_n\bar{p}_n-a_n\bar{u}_{n-1}-\lambda_n a_n\bar{p}_{n-1}=f_n$$

$$b_n\bar{u}_{n+1}-\lambda_n b_n\bar{p}_{n+1}+\bar{u}_n-\lambda_n\bar{p}_n-b_n\bar{u}_{n-1}+\lambda_n b_n\bar{p}_{n-1}=g_n$$

$$k_n\bar{S}_{n+1}+\bar{S}_n-k_n\bar{S}_{n-1}=S_n$$

where bars refer to quantities at the new time level, and

$$a_n=\frac{\tau}{2\Delta x'}\left[(u_n+c_n)(\mathrm{FAC})-v_n\right]$$

$$b_n=\frac{\tau}{2\Delta x'}\left[(u_n-c_n)(\mathrm{FAC})-v_n\right]$$

$$k_n=\frac{\tau}{2\Delta x'}\left[u_n(\mathrm{FAC})-v_n\right]$$

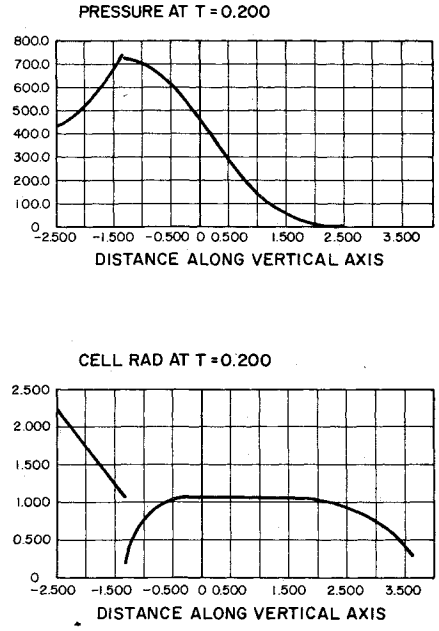

Fig. 8 Pressure profile and cavity shape. Depth = 0.26, T = 0.2.

$$\mathrm{FAC}=1-\frac{dv}{dx}\delta t$$

$$\lambda_n=\frac{1}{\rho_n c_n}$$

$$f_n=-\frac{u_n c_n\tau}{Q_n}\frac{\partial Q_n}{\partial x}-\frac{c_n\tau}{Q_n}\frac{\partial Q_n}{\partial t}+u_n+\lambda_n p_n$$

$$v_n=\text{velocity of grid point}=\frac{\bar{r}_n-r_n}{\tau}$$

$$g_n=\frac{u_n c_n\tau}{Q_n}\frac{\partial Q_n}{\partial x}+\frac{c_n\tau}{Q_n}\frac{\partial Q_n}{\partial t}+u_n-\lambda_n p_n$$

Boundaries and the double sweep procedure are executed as in Godunov's two step method.

A smoothing interpolation is now carried out to solve for the values of the variables at the half integral position, $n+\frac{1}{2}$. The purpose of this operation is to dampen grid point to grid point oscillations which sometimes appear. As mentioned before, the model equation is found to be unconditionally stable. However, in the actual numerical scheme for the characteristic equations of motion, grid to grid oscillations in the variables occur for certain geometries and equations of state. Specifically, for the spherically symmetric geometry, and the Tait equation of state for water, the scheme seemed particularly vulnerable to oscillations. These oscillations did not decrease as the time step was decreased. Consequently, the variables after each time step were interpolated according to the following formula

$$\bar{f}_{n+\frac{1}{2}}=(1-\alpha)(\psi_{n+\frac{1}{2}}\bar{f}_n+v_{n+\frac{1}{2}}\bar{f}_{n+1})$$

$$+\alpha(\phi_{n+\frac{1}{2}}\bar{f}_{n-1}+\chi_{n+\frac{1}{2}}\bar{f}_{n+2})$$

where

$$\psi_{n+\frac{1}{2}}=(\bar{r}_{n+1}-\bar{r}_{n+\frac{1}{2}})/(\bar{r}_{n+1}-\bar{r}_n)$$

$$\phi_{n+\frac{1}{2}}=(\bar{r}_{n+2}-\bar{r}_{n+\frac{1}{2}})/(\bar{r}_{n+2}-\bar{r}_{n-1})$$

$$v_{n+\frac{1}{2}}=(\bar{r}_{n+\frac{1}{2}}-\bar{r}_n)/(\bar{r}_{n+1}-\bar{r}_n)$$

$$\chi_{n+\frac{1}{2}}=(\bar{r}_{n+\frac{1}{2}}-\bar{r}_{n-1})/(\bar{r}_{n+2}-\bar{r}_{n-1})$$

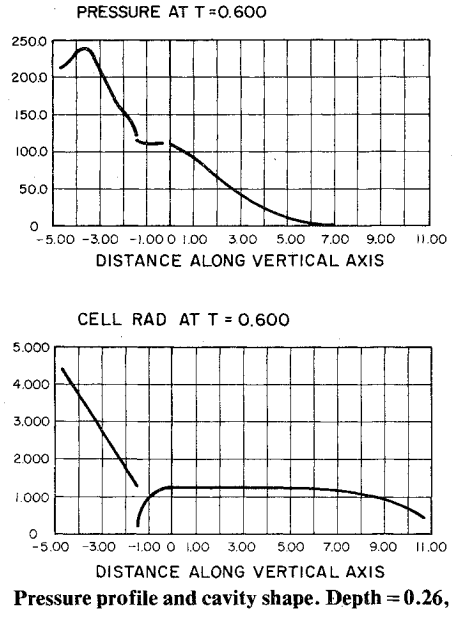

Fig. 9 Pressure profile and cavity shape. Depth = 0.26, $T = 0.6$.

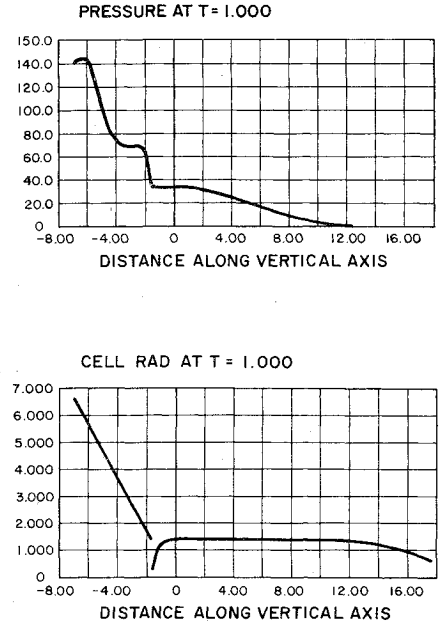

Fig. 10 Pressure profile and cavity shape. Depth = 0.26, $T = 1.0$.

α is a parameter taken to be 0.25. This interpolation eliminated the oscillations.

In summary, the basic formulation for the numerical program used was taken from the first step of Godunov's 1970 scheme. This work was then extended to the case of time dependent streamtube cross-sectional area. An additional term was added to the equations to compensate for the violently deforming grid network in the upper critical depth problem. The method is implicit and stable for any time step desired.

Results

The results of the numerical calculations are presented in Figs. 8-11. The radius of the cavity is taken to be of unit length. Pressure is shown in atmospheres. In a given unit of nondimensional time, a sound wave in sea level air would travel 1.183 units of length. The units of dimensionless impulse are just

$$[I] = [p]\ [L]^2\ [T]$$

where brackets denote dimensions, p is pressure in atmospheres, L is the nondimensional length, and T is the nondimensional time. For a unit length of 1 meter the time unit is 3.56×10^3 sec.

Figures 8-10 show the evolution of the pressure profile and of the cavity shape for a particular depth of placement = 0.26, as the chimney section takes form and grows. During this period the pressure inside the cavity is being released quite rapidly by the venting of gas out through the chimney region. At the bottom of the cavity the pressure is decreasing because the cavity is expanding into the water. The pressure profile in water has a peak in all cases shown. The pressure increase between the water shock and the peak on the pressure profile is accelerating the fluid particles which have been overtaken by the water shock. At the same time the decreasing pressure inside the cavity is decelerating the water between the pressure peak and the contact discontinuity. The pressure pulse formed by this maximum propagates up to the shock, and Fig. 10 shows the formation of another peak. (The diagonal lines in the cavity diagrams show the shock radius.)

Figure 11 shows the variation of impulse/time with time for the same depth of placement. The impulse/time initially decreases and then increases to its maximum. This early drop in impulse is due to the upward propagation of the weak rarefaction wave from the bottom of the cavity through the

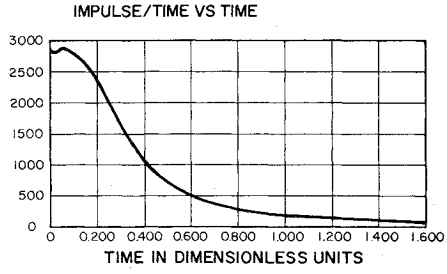

Fig. 11 Impulse/time variation with time. Depth = 0.26, Total Impuse = 1204.

cavity region. However, by time $T = 0.04$ the influence of the stronger rarefaction wave resulting from the venting of the hot gas begins to decrease the pressure inside the lip region, or intermediate region, of the cavity. As the pressure above the hemisphere is relieved, the applied impulse increases until its maximum occurs at $T = 0.06$. After that time the strong rarefaction begins to decrease the pressure pushing down against the water. Also, by $T = 0.2$ the chimney walls have grown to the same radius as the hemisphere (see Fig. 9). Thus the impulse imparted to the water will decrease smoothly as a function of time.

The least certain aspect of the physical model is how the chimney develops and expands in time. The calculations of Bjork and Gittings[3] were performed for a depth of placement equal to the radius of the charge. As can be seen from their work, the water constrains the venting gases to move mostly in the vertical direction. In the present model the vertical venting assumption probably is not very accurate for depths of placement as small as 0.26. In this range the expansion would be closer to spherical in character rather than linear. Hence a plot of impulse/time would drop faster after it has reached its peak value than is shown in Fig. 11. Also, the total impulse applied for this depth would be smaller.

Further work on the behavior of the cavity should include a geometry for the chimney which would simulate an approximate spherical expansion of the hot gas products as they vent into the atmosphere. This would increase the accuracy of the present model as the depth of placement goes to zero.

The results were calculated on the Lawrence Berkeley Laboratory CDC 7600 computer with a running time of 1 min for each complete case.

Conclusions

By means of the model developed in this paper we have been able to predict impulse/time as a function of time for a variety of depths of placement. Work is currently in progress to use the results generated by the model to initiate a calculation of the actual wave forms. When this is completed actual comparisons may be made between the performance of the model and experiment.

References

[1]Sakurai, A., "Upper Critical Depth Wave Generation," Rept. N-72-1, March 1972, U.S. Army Engineer Waterways Experimental Station, Vicksburg, Miss.

[2]Sedov, L. I., *Similarity and Dimensional Methods in Mechanics* (English translation edited by M. Holt), Academic Press, N.Y., 1959, pp. 210-238.

[3]Bjork, R. L. and Gittings, M. L., "Wave Generation by Shallow Underwater Explosions," Rept. 1009, Dec. 1972, Systems, Science, and Software, LaJolla, Calif.

[4]Alalykin, G. B., Godunov, S. K., Kireeva, I. L., Pliner, L. A., "Solutions of One Dimensional Problems in Gas Dynamics with Movable Networks," (In Russian) NAUKA, Moscow, 1970.

[5]Rosen, S. M., "Numerical Solution to Water Waves Produced by Explosions," University of California, Berkeley Rept. FM-74-11, Sept. 1974, Berkeley, Calif.

[6]Whitham, G. B., *Linear and Non-linear Waves*, Wiley, N.Y., 1974.

[7]Friedman, M. P., "A Simplified Analysis of Spherical and Cylindrical Blast Waves," *Journal of Fluid Mechanics*, Vol. 11, 1961, pp. 1-15.

[8]Ballhaus, W. F., Jr. and Holt, M., "Interaction Between the Ocean Surface and Underwater Spherical Blast Waves," *Physics of Fluids*, Vol. 17, 1974, pp. 1068-1079.

[9]Chan, B. C., Holt, M., and Welsh, R. L., "Explosions Due to Pressurized Spheres at the Ocean Surface," *Physics of Fluids*, Vol. 11, 1968, pp. 714-722.